NMR and Dipole Moment Investigation of the Conformational Distribution in a Liquid Crystal Forming Polymer Containing an Asymmetric Carbon in the Flexible Spacer

Nicholas J. Heaton, Pablo Bello, A. Bello, and Evaristo Riande*

Instituto de Ciencia y Tecnología de Polímeros (CSIC), Juan de la Cierva 3, 28006 Madrid, Spain

Received June 9, 1997[⊗]

ABSTRACT: The conformational distribution of the main chain liquid crystal polymer, poly(3-((methyltrimethylene)oxy)trimethylene *p,p′*-bibenzoate) has been studied in solution by analysis of NMR vicinal coupling constants and the dipole moment. Analysis of the temperature dependence of the coupling constants for the methylene groups adjacent to the asymmetric carbon in the glycol spacer, measured between −45 °C and 45 °C, yields values for the conformational energies for each of the bonds flanking the asymmetric carbon. Spectra recorded in deuterated chloroform and 1,4-dioxane-d_8 yield similar values for the coupling constants, indicating that solvent polarity does not significantly influence the conformational distribution. Because of uncertainty in the assignment of NMR signals, two sets of energies are obtained for each bond. This ambiguity is partly resolved by analysis of the dipole moment. An experimental value of 0.73 is obtained for the dipolar correlation coefficient, g, in dioxane at 30 °C, which is consistent with energies $E_{\sigma\beta} = 0.5 \pm 0.3$ kJ mol^{-1} and $E_{\sigma\alpha} = -1.3 \pm 0.4$ kJ mol^{-1} for the bond adjacent to the ether linkage. Tentative values of $E_{\sigma\alpha p} = 0.0 \pm 0.30$ and $E_{\sigma\beta p} = 1.1 \pm 0.4$ kJ mol^{-1} are obtained for the neighboring bond attached to the ester group, based on the NMR analysis and comparison with conformational energies in poly(3-methyloxetane), which possesses a similar structural unit.

1. Introduction

The rotational isomeric state (RIS) model has proved to be an important tool for the theoretical evaluation of conformation dependent properties of molecular chains as a function of their structure.[1,2] Equilibrium dielectric properties, such as the mean-square dipole moments, random-coil dimensions, for example, the mean-square end-to-end distance and radius of gyration, and optical properties, such as the Kerr effect and the optical configuration parameter, have been calculated using the RIS model for a variety of polymers, and the results obtained are generally in satisfactory agreement with the experiment.[3,4]

The prediction of conformational properties of polymer chains generally requires knowledge of the first- and second-order conformational energies arising, respectively, from rotations about a single bond and from rotations about pairs of consecutive bonds. Relative values of the conformational energies associated with the skeletal bonds of polymer chains are usually obtained from the analysis of spectroscopic or thermodynamic data for low molecular weight compounds whose conformational characteristics are similar to those of the polymers.[5,6] Comparison of experimental and theoretical values of conformation-dependent properties provides reliable estimates for the relative energies. Among the methods used to determine conformational energies, dipole moment studies and NMR spectroscopy stand out. Both approaches have been applied extensively to the investigation of conformational behavior of oxygen-containing chains. Dipole moments are sensitive, in principle, to conformational energies and geometries of all bonds in the polymer chains. In contrast, vicinal coupling constants, J, measured by NMR spectroscopy, reflect conformational distributions about specific bonds.[7] The two methods are then complementary, and by combining evidence from both techniques, it is possible to estimate conformational energies even in relatively complex chains.

According to the RIS approach, dipole moments and vicinal coupling constants are regarded as equilibrium averages over a limited number of conformers, defined by the torsion angles, ϕ, for each skeletal chain bond, valence angles and bond lengths being assigned fixed values. The allowed conformers are identified with minima in the intramolecular potentials. For linear all-methylene and ether chains, each bond assumes one of the three alllowed conformations, trans (t), gauche+ (g^+) and gauche− (g^-). Within the scope of the RIS model, dipole moments then depend only on the conformational energies, individual bond (or group) dipoles, and the particular values for the ϕ. For most esters and ether linkages, good estimates for the individual bond or group dipoles are available, while the torsion angles are known to vary relatively little from the standard values of 0, +120, and −120° for t, g^+, and g^- states, respectively. Indeed, in some cases it is sufficient to regard both the group dipole moments and the individual torsion angles as fixed parameters so that the only unknown quantities for evaluating dipole moments using the RIS model are the conformational energies. Nevertheless, for chains comprising several different types of bonds, many independent conformational energies may be required, whereas experimental studies provide just a single quantity, the mean square dipole moment, at each temperature. Fortunately, the vast literature of conformational studies of hydrocarbon and polyether chains provides reliable values for the conformational energies of many types of chain linkage which may be adopted for the purposes of investigating more complex chain segments.

A similar approach is followed for the RIS analysis of vicinal coupling constants. In this case, the unknown quantities are the conformational energies and the J values for individual conformers. These quantities, which are very sensitive to molecular structure and geometry, are generally not known *a priori* and it has

[⊗] Abstract published in *Advance ACS Abstracts,* November 15, 1997.

S0024-9297(97)00813-9 CCC: $14.00

usually been necessary to make further assumptions in order to proceed with a meaningful analysis. A number of different philosophies have been adopted in this respect. In their investigation of poly(ethylene oxide) and model compounds, Matsuzaki and Ito[8] proposed a simple empirical relationship between the individual conformer coupling constants and performed the fitting procedure with a reduced number of parameters. This allowed good fits to experimental data to be obtained, but the resulting values for the individual coupling constants fell considerably outside the usual range of values expected for these quantities. An alternative approach, which has been adopted by several groups[9−11] makes use of modified versions of the Karplus equation[12,13] to determine values for the conformer coupling constants, assuming fixed values for the torsion angles in each conformation. The temperature dependence of the observed couplings is then fit by varying only the conformational energies. This procedure ensures that all the fitting parameters maintain physically reasonable values but in some cases imposes overstringent restrictions on the various coupling constants, which could have a significant effect on the resulting conformational energies. Tasaki and Abe have discussed the different fitting approaches[14] in reference to their work on poly(oxyethylene) and 1,2-dimethoxyethane.[15,16] They chose to retain all independent coupling constants as free parameters and performed best fits to their data as a function of E_σ, the energy of the gauche conformation about the C−C bond. This approach is certainly reasonable since it provides an internal indication of the validity of the fitting procedure. Limiting values for the conformational energies can then be obtained by considering only physically reasonable values for the coupling constants. Specific values for the energies could be derived by placing limits on the relative magnitudes of individual coupling constants. In view of the different approaches adopted by various research groups and the vastly different values employed for conformational coupling constants in identical compounds, it is somewhat surprising that results for conformational energies are often in semiquantitative agreement. This observation, however, would appear to support the use of the NMR coupling constant method as a valid and reliable technique for investigating conformation in flexible chains.

This work forms part of a general study of the influence of single asymmetric carbon atoms on the conformational properties of flexible ether spacer chains and how this, in turn, may condition the development of mesophases in main chain polyesters. A considerable body of work has now been published concerning the role of linear spacer chains on the behavior of polymeric as well as low molecular weight liquid crystals. It is well established that the mesogenic behavior of these materials hinges on the combination of the inherently anisotropic molecular interactions of the rigid core units and the relative disposition of these units, which is dictated by the structure of the spacer chain connecting them. Indeed, several molecular theories have now been proposed which successfully account for the thermodynamic properties and orientational order of liquid crystals and main chain liquid crystal polymers with linear spacers.[17,18] Relatively little attention, however, has been paid to the effects of asymmetric centers on the conformational properties of liquid crystals, despite the fundamental role they play in governing the ferroelectric properties, which are important for the design of optical devices.[19,20] In this study, the conformational energies of the $OCH_2CH(CH_3)CH_2O$ residue in poly(3-((methyltrimethylene)oxy)trimethylene *p,p′*-bibenzoate) (PTOMTB) are investigated by NMR and dipole moment measurements. Section 2 contains a description of the experimental details and materials used. In section 3, an account is given of the RIS analysis of the NMR coupling constant data and the results of this analysis are then considered with reference to the dipole moment analysis of the polymer.

2. Experimental Part

Synthesis of Poly(3-((methyltrimethylene)oxy)trimethylene *p,p′*-bibenzoate). PTMOTB was synthesized by transesterification of 3-((methyltrimethylene)oxy)trimethylene glycol and diethyl *p,p′*-bibenzoate, respectively, using isopropyl titanate as catalyst. The polymer was purified by precipitating into methanol its chloroform solution. Its structure was confirmed by ^{1}H and ^{13}C NMR spectroscopy. The value of the intrinsic viscosity of PTOMB, measured at 25 °C in chloroform, was 0.54 dL/g.

NMR Measurements and Spectral Analysis. The ^{1}H vicinal coupling constants for PTMOTB were derived from NMR spectra recorded on Varian INOVA 300 and UNITY 500 spectrometers. Spectra were obtained at several temperatures from −45 to +45 °C for PTMOTB solutions in deuterated chloroform and from 20 to 80 °C for solutions in deuterated dioxane. Vicinal coupling constants for the $OCH_2CH(CH_3)$-CH_2O segment methylene groups were obtained by fitting the experimental spectra with simulated line shapes based on standard expressions for the line frequencies for ABX spin systems.[21] A FORTRAN program was developed for this purpose that employs a nonlinear least squares fitting routine in which the coupling constants, J_{AB}, J_{AX}, and J_{BX}, the chemical shifts for spins A, B, and X, and the respective line widths are varied independently. The resulting best fit coupling constants are estimated to be accurate to within 0.1 Hz.

Dipole Moments. The static dielectric permittivity ϵ of dioxane solutions of PTMOTB was measured at 30 °C with a capacitance bridge (General Radio, type 1620 A) coupled with a three terminal cell. The measurements were performed at 10 kHz, at which the real component, ϵ', of the complex dielectric permittivity coincides with the static dielectric permittivity. The values of ϵ were plotted against the weight fraction w of solute, and from the slope of the plot in the limit $w \rightarrow 0$, the term $d\epsilon/dw$ proportional to the total polarization (orientation, electronic, and atomic) was obtained. Values of the increment of the index of refraction n of the solutions with respect to that of the solvent n_1 were measured with a differential refractometer (Chromatix, Inc). The values of Δn were plotted against w, and from the slope in the limit $w \rightarrow 0$, the term dn/dw, proportional to the electronic polarization, was determined. The atomic polarization is in most cases only a very small percentage of the electronic polarization and because of the small value of the latter it was considered to be negligible. Values of $d\epsilon/dw$ and dn/dw for PTMOTB are 3.06 and 0.15, respectively. The mean-square dipole moment, $\langle\mu^2\rangle$, of the polymer was evaluated by the method of Guggenheim and Smith:[22,23]

$$\langle\mu^2\rangle = \frac{27k_BTM}{4\pi\rho N_A(\epsilon_1+2)^2}\left[\frac{d\epsilon}{dw} - 2n_1\frac{dn}{dw}\right]$$

where k_B and N_A are respectively the Boltzmann constant and Avogadro's number, M is the molecular weight of the solute, ρ is the density of the solvent and n_1 and ϵ_1 are, respectively, the index of refraction and the permittivity of the solvent. The value of $\langle\mu^2\rangle$ obtained for PTMOTB at 30 °C is 7.70 ± 0.20 D^2.

3. Results and Analysis

(a) Vicinal Coupling Constants. Figure 1 shows the molecular structure and proton NMR spectrum of PTMOTB in $CDCl_3$ at 318 K. The protons in each of

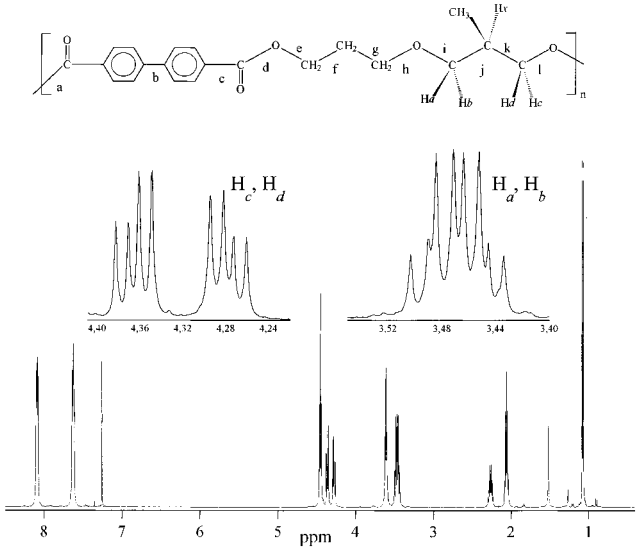

Figure 1. Molecular structure (showing bond labels) and 500 MHz ^{1}H NMR spectrum of PTMOTB at 318 K. Insets show expanded sections corresponding to the methylene groups adjacent to the asymmetric carbon.

Table 1. Vicinal Coupling Constants for PTMOTB

T (K)	J_{AX} (Hz)	J_{BX} (Hz)	$J_{A'X}$ (Hz)	$J_{B'X}$ (Hz)
		Measured in $CDCl_3$		
228	5.65	7.33	6.13	5.71
243	5.64	7.06	6.09	5.78
258	5.63	6.79	6.08	5.84
273	5.62	6.64	6.06	5.87
288	5.61	6.60	6.06	5.89
303	5.64	6.50	6.08	5.96
318	5.63	6.49	6.11	5.98
		Measured in 1,4-Dioxane-d_8		
298	5.61	6.38	6.09	6.06
308	5.65	6.35	6.10	6.07
323	5.69	6.29	6.10	6.05
338	5.73	6.26	6.08	6.09
353	5.82	6.20	6.09	6.07

the methylene groups adjacent to the $-CHCH_3-$ asymmetric center are magnetically inequivalent and present ABX multiplets (see expanded sections in Figure 1) due to coupling with the methine proton. Analysis of the multiplets yields values for the chemical shifts for each proton, the geminal (J_{AB}) and vicinal (J_{AX} and J_{BX}) coupling constants. The vicinal coupling constants, measured from 328 to 318 K in $CDCl_3$ and from 293 to 253 K in 1,4-dioxane-d_8, are given in Table 1 and plotted in Figure 2.

In the remaining discussion we arbitrarily label the downfield resonances in each ABX multiplet as spin A signals and the upfield resonances as spin B signals. Since the proton chemical shifts are themselves conformation dependent, as well as being sensitive to remote substituents, it is not possible, *a priori*, to assign resonances A and B to specific protons. Thus, in the case of the methylene group attached to the ether linkage, spin A may correspond to either proton a or proton b (see Figure 1) and likewise for spin B. The same argument also applies for the assignment of spins A′ and B′ to protons c and d in the methylene group attached to the ester group.

Before embarking on a detailed analysis of the data, it is possible to make some general comments concerning these results. First, the coupling constants appear to vary little with the polarity of the solvent. This observation is in keeping with results obtained for

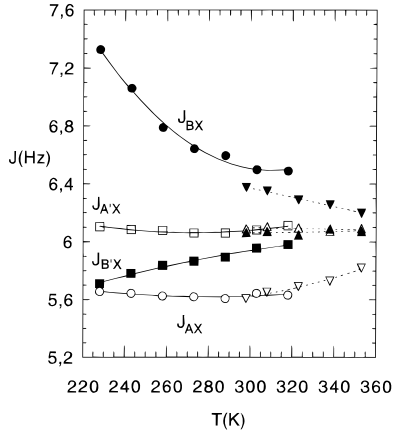

Figure 2. Experimental vicinal coupling constants recorded in $CDCl_3$ and dioxane-d_8 for methylene groups adjacent to the asymmetric carbon atom in the glycol...spacer of PTMOTB. Results obtained in $CDCl_3$ are J_{BX} (filled circles), J_{AX} (open circles), corresponding to protons a and b, and $J_{B'X}$ (filled squares), $J_{A'X}$ (open squares) corresponding to protons c and d. Results obtained in dioxane-d_8 are J_{BX} (filled inverted triangles), J_{AX} (open inverted triangles) and $J_{B'X}$ (filled upright triangles), $J_{A'X}$ (open upright triangles). Solid and broken lines are intended purely as guides for the eye.

diesters containing ether spacer chains[11] and suggests that the conformational behavior of these materials is little influenced by the dielectric constant of the surrounding solvent. We note that somewhat larger variations in coupling constants with solvent polarity have been observed for poly(oxyethylene).[14] However, in this case, hydrogen bonding between solvent (for example, D_2O) and solute molecules is possible and this is likely to play a significant role in stabilizing certain conformations. In the remainder of this analysis, we concentrate on the results obtained in $CDCl_3$, which provide a broader temperature range. Regarding the temperature dependence of the coupling constants, only J_{BX} varies substantially over the temperature range studied. In addition, $J_{A'X}$ and $J_{B'X}$ adopt rather similar values, falling between 5.5 and 6.0 Hz over the range studied in $CDCl_3$. From this observation we can immediately infer that the energy differences between the different conformers for bonds of type k (see Figure 1) are relatively small. Conversely, the rather large values (6.5−7.3 Hz) for J_{BX} and its pronounced temperature dependence indicate appreciable differences in the conformational energies for bond type j.

Conformational Analysis. Figure 3 shows projections of each of the conformations for the two relevant $-C-C-$ bonds, indicating the various coupling constants for each conformer. In the present analysis, we consider only first-order interactions. The energies $E_{\sigma\alpha}$ and $E_{\sigma\beta}$, for the gauche states of bond j relative to that of the trans state and the equivalent quantities, $E_{\sigma\alpha p}$ and $E_{\sigma\beta p}$, for bond k are independent. These values, together with their specific assignment to the g^+ and g^- states, completely define the conformational distribution for bonds j and k. This approximation neglects possible higher order interactions involving the ester group and other methylene groups in the spacer. In principle, coupling constants for consecutive $-C-C-$ bonds (e.g., bonds j and k) may be sensitive to correlation between the successive torsion angles. However, in the present case, it may be shown (see section below on *higher order interactions*) that the coupling constants of interest are governed principally by the first-order interactions. Within the framework of this approxima-

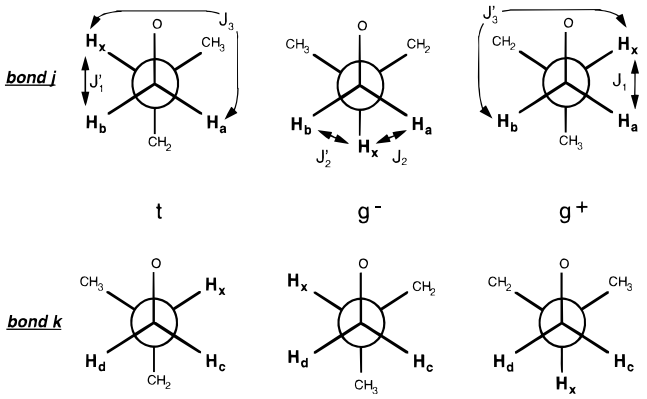

Figure 3. Projections of trans (t), −gauche (g^-), and +gauche (g^+) for bonds j and k in PTMOTB. Also shown are individual coupling constants J_1, J'_1, J_2, J'_2, J_3, and J'_3 for bond j. A similar set of coupling constants may be defined for the corresponding interactions in bond k.

tion, the effective coupling constants for protons a and b are

$$J_{ax} = f^j_{(+)}J^j_1 + f^j_{(-)}J^j_2 + f^j_{(t)}J^j_3 \quad (1a)$$

$$J_{bx} = f^j_{(-)}J'^j_3 + f^j_{(+)}J'^j_2 + f^j_{(t)}J'^j_1 \quad (1b)$$

where $f^j_{(t)}$, $f^j_{(+)}$, and $f^j_{(-)}$ are the populations of the t, g^+, and g^- states, states for bond j. The coupling constants, J^j_N and $J^{j'}_N$ (N = 1,2,3) are, in general, independent, governed by the geometry of each conformation. Although the effective coupling constants in eq 1 correspond to the measured quantities, J_{AX} and J_{BX}, no assignment of protons a and b with respect to spins A and B has yet been made. Similarly, for bond type k we have

$$J_{cx} = f^k_{(-)}J^k_2 + f^k_{(+)}J^k_3 + f^k_{(t)}J^k_1 \quad (2a)$$

$$J_{dx} = f^k_{(-)}J'^k_2 + f^k_{(+)}J'^k_1 + f^k_{(t)}J'^k_3 \quad (2b)$$

which correspond to the measured couplings, $J_{A'X}$ and $J_{B'X}$, bearing in mind that no specific assignment has yet been made for spins A′ and B′.

The conformer populations for bond j are given by the respective Boltzmann factors,

$$f^j_{(\nu)} = \frac{\exp(-E^j_{(\nu)}/RT)}{\sum_\mu \exp(-E^j_{(\mu)}/RT)} \quad (3)$$

where $E^j_{(\mu)}$ is the energy of conformer μ for bond j relative to that of the corresponding trans conformation. Thus, we have $E^j_{(t)} = 0$ and the gauche state energies, $E^j_{(+)}$ and $E^j_{(-)}$, adopt the values $E_{\sigma\alpha}$ and $E_{\sigma\beta}$, following the usual convention $E_{\sigma\alpha} < E_{\sigma\beta}$. An analogous expression is obtained for bond k. There are eight independent quantities which determine the two measured coupling constants for each bond—six coupling constants, J^j_i and J'^j_i, i = 1−3, and the two energies, $E^j_{(+)}$ and $E^j_{(-)}$. In order to progress further with the analysis, we now make the approximation $J'^j_i = J^j_i$. A similar approach was adopted by Tasaki and Abe[14] to facilitate their analysis of coupling constant data for 1,2-dimethoxyethane. For the present case, the approximation is certainly reasonable provided that the dihedral angles in each of the conformations do not deviate too much from the *standard* values, 0, and ±120°.

Bond j. The model outlined above provides the coupling constants, J_{ax} and J_{bx}, as a function of J^j_1, J^j_2, J^j_3, $E^j_{(+)}$, and $E^j_{(-)}$. Fits to the experimental coupling constant data have been carried out, varying J^j_1, J^j_2, $E^j_{(+)}$, and $E^j_{(-)}$ for different fixed values of J^j_3. This procedure was adopted since the trans coupling constants, J_3, are relatively insensitive to the dihedral angle between the coupled protons and previous studies of vicinal coupling constants indicate that J_3 are of the order 11.5 ± 2.0 Hz.[13] During the fitting procedure, limits are placed on the values of J^j_1 (1.0−7.0 Hz) and J^j_2 (1.0−5.0 Hz) to ensure that these quantitites maintain physically realistic values. Because of the ambiguity in the assignment of the resonances, it is necessary to repeat the fitting procedure for each of the two possible combinations, A ≡ a, B ≡ b (case 1) and A ≡ b, B ≡ a (case 2). However, the symmetry imposed on the model by the coupling constant approximation, $J^j_i = J'^j_i$, implies that the two cases are related by a simple exchange of relative energies for the g^+ and t conformers. The best fit values for the coupling constants and the quality of the resulting fits are unchanged. Figure 4 shows the best fit values for the coupling constants and energies as a function of J^j_3. For both case 1 and case 2, $E^j_{(-)} > E^j_{(t)}$, indicating the presence of unfavorable interactions between the oxygen atom of the ether linkage and the methyl and methylene groups in the gauche orientations. The major difference between the two assignments lies in the absolute value of $E^j_{(+)}$. For case 1, we have 0.5 kJ mol^{-1} < $E^j_{(+)}$ < 1.5 kJ mol^{-1}, whereas for case 2, the g^+ state is found to be of lower energy, −1.5 kJ mol^{-1} < $E^1_{(+)}$ < −0.5 kJ mol^{-1}. Were it not for Coulombic interactions, the g^+ and trans states should be expected to have similar energies. However, charge separation in C−O bonds leaves charges $\delta+$ and $\delta-$ respectively on the carbon and oxygen atoms which would lead to favorable Coulombic interactions between C and O atoms in gauche orientations. This argument is consistent with case 2, which yields a negative value of $E^1_{(+)}$. The best fit coupling constant profiles, obtained with J^j_3 = 11.5 Hz, are shown in Figure 5. Profiles corresponding to different J^j_3 values are virtually identical. Despite the large number of variable parameters in the model, systematic differences remain between the best fit profiles and experimental results. In particular, the pronounced temperature dependence of J_{BX} and its rather large value at low temperatures, are not adequately reproduced by the model. The discrepency must derive either from the approximations concerning the relative magnitudes of the individual coupling constants or from the neglect of higher order interactions in the RIS model employed in the analysis. The former possibility has been investigated by considering more explicitly the geometrical constraints on the coupling constants. Altona and co-workers[13] have developed a useful empirical expression for vicinal coupling constants in C−C bonds as a function of the dihedral angles and the electronegativity of each substituent. We have used this expression to evaluate individual coupling constants as a function of conformation of bond j. The resulting profiles are plotted in Figure 6. The angle, Φ, is the torsion angle between the ether oxygen atom and the methylene group, which defines the conformational state of the bond. In evalu-

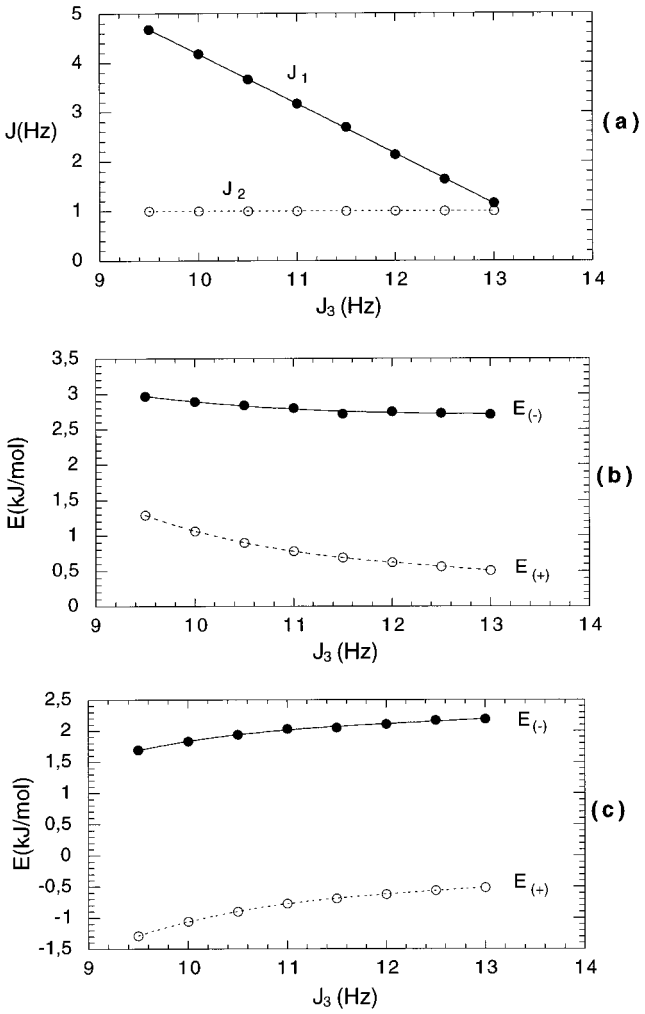

Figure 4. (a) Individual coupling constants, J_1 and J_2, as a function of J_3 obtained by fitting the temperature dependence of J_{AX} and J_{BX}. Results correspond to either assignment case 1 (spin A → proton a, spin B → proton b) or case 2 (spin A → proton b, spin B → proton a). (b) Energies of g^+ and g^- states for bond j as a function of J_3 obtained from the fitting procedure, assuming the case 1 assignment. (c) Energies of g^+ and g^- states for bond j as a function of J_3 obtained from the fitting...procedure, assuming the case 2 assignment.

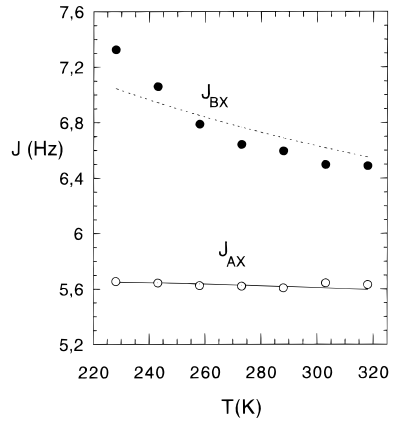

Figure 5. Best fit profiles for J_{AX} and J_{BX} obtained using the "model free" approach. Filled circles and broken lines refer to experimental and best fit J_{BX} values, respectively. Open circles and solid lines refer to experimental and best fit J_{AX} values. Best fit profiles for cases 1 and 2 are indistinguishable.

ating these profiles it has been assumed that the difference in the dihedral angles, $\Phi_{bx} - \Phi_{ax}$ (see Figure 3), is constant at 120°. While this condition is not

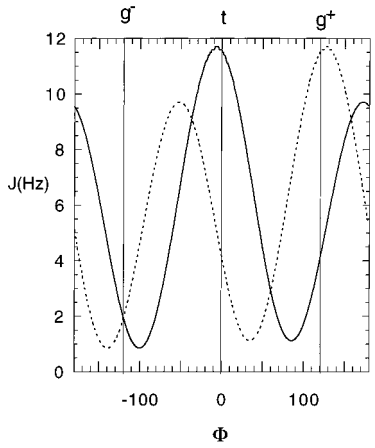

Figure 6. Torsion angle dependence of coupling constants J_{ax} (solid lines) and J_{bx} (broken lines) evaluated according to the empirical model (see text). Profiles shown correspond to bond j (see Figure 3). Profiles for bond k are related to those shown here by reflection about the $\Phi = 0$ line with J_{dx} replacing J_{ax} and J_{cx} replacing J_{bx}.

expected to be satisfied rigorously for all Φ, substantial deviations from the approximation are unlikely since this would require significant variations in the HCH bond angle and concomitant large increases in energy.

The experimental coupling constants have been fit using the first-order RIS model with energies $E^j_{(+)}$ and $E^j_{(-)}$ and torsion angles $\Phi_{(t)}$, $\Phi_{(+)}$, and $\Phi_{(-)}$ as variable parameters by applying the empirical expression to obtain the individual coupling constants, J^j_i and J'^j_i, for each conformer. The fitting procedure was repeated for different values of $\Delta\Phi$, the maximum allowed deviation of the conformation torsion angles, $\Phi_{(t)}$, $\Phi_{(+)}$, and $\Phi_{(-)}$, from their *standard* values of 0, +120, and −120°. The results obtained for both assignment cases are plotted in Figure 7. As should be expected, the ranges of values obtained for $E^j_{(+)}$ and $E^j_{(-)}$ are comparable to those obtained using the model free approach (see Figure 4). For case 1 we obtain $E^j_{(-)} = E_{\sigma\beta} = 2.0 \pm 0.6$ kJ mol^{-1} for the g^- state and $E^j_{(+)} = E_{\sigma\alpha} = 1.4 \pm 0.4$ kJ mol^{-1} for g^+. The best fit values for case 2 are $E^j_{(-)} = E_{\sigma\beta} = 0.5 \pm 0.3$ kJ mol^{-1} and $E^j_{(+)} = E_{\sigma\alpha} = -1.3 \pm 0.40$ kJ mol^{-1}. The variation in the torsion angles is shown in Figure 7c,d. In view of the rather crude model used to describe the bond geometry (e.g., no variation in bond angles, a fixed value of 120° for the difference in torsion angles for geminal protons) and possible inaccuracies in the simple empirical model employed for the angle dependence of the coupling constants, these values of Φ obtained should be regarded only as very approximate estimates. Nevertheless, it is reasonable to assume that large deviations of Φ from their standard values correspond to significant distortions of the bond from its ideal geometry, reflecting strong intramolecular nonbonded interactions. Conversely, small deviations indicate the absence of such interactions. Within the bounds of this model, all distortions of bond geometry are associated with deviations in the dihedral angle, Φ, describing bond conformation. Presumably, the overall distortion should be distributed among all bond angles and bond lengths in the unit so that the correct values of Φ may be significantly closer to their standard values than those indicated by the model. This approach is useful since it guarantees physically realistic values for the coupling constants while providing an indication of the corresponding bond geometry. On increasing $\Delta\Phi$, successively better fits are obtained to the experimental

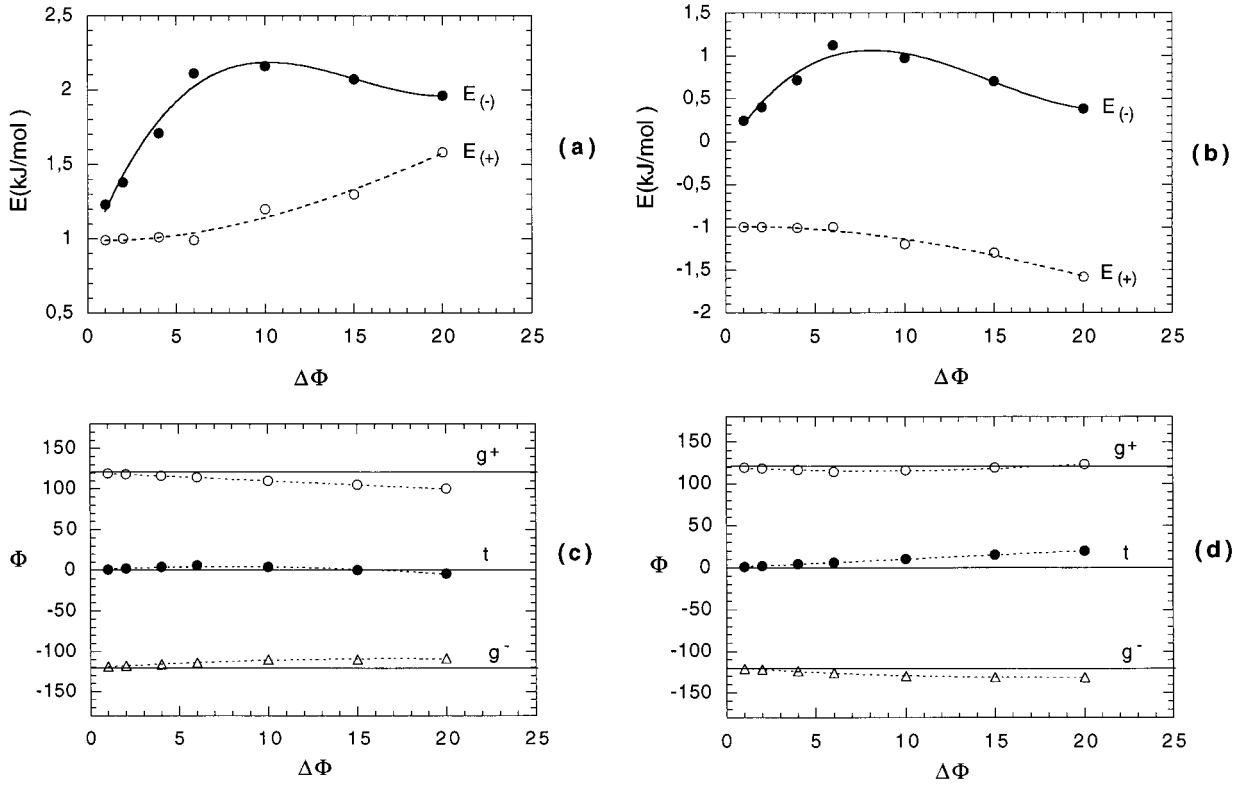

Figure 7. Best fit values of conformational energies, $E_{(+)}$ and $E_{(-)}$, as a function...maximum torsion angle distortion, $\Delta\Phi$, for bond j, assuming (a) case 1 and (b) case 2 NMR assignments. Below are shown best fit values for t, g^+, and g^- torsion angles for bond j assuming (c) case 1 and (d) case 2.

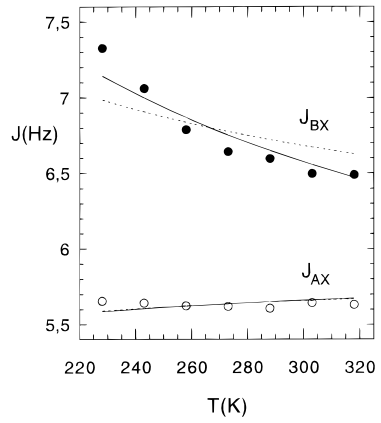

Figure 8. Best fit profiles for J_{AX} and J_{BX} for bond j obtained using the empirical model approach (see text). Filled circles and open circles refer to experimental values for J_{BX} and J_{AX}, respectively. Broken lines were obtained with $\Delta\Phi = 1°$. Solid lines are the best fit profiles with $\Delta\Phi = 15°$.

coupling constant profiles. This effect is illustrated by the example best fit profiles shown in Figure 8. For $\Delta\Phi = 15°$, the quality of the calculated profiles is significantly better than that provided by the model free approach. Comparison of the torsion angle plots (Figure 7c,d) provides a simple physical interpretation of the differences between the two assignment cases. For case 1, the greatest distortion is observed for the g^- state, whereas in case 2, it is the trans configuration that is most distorted. However, in order to resolve the ambiguity in assignment, further experimental evidence is required (see section on dipole moment analysis).

Bond k. The same first-order conformational analysis has been applied to interpret the vicinal coupling constants, $J_{A'X}$ and $J_{B'X}$, for protons c and d. As before, the "model-free" approach and the empirical model provide similar values for the conformational energies in each of the two possible assignment cases, A′ ≡ c, B′ ≡ d (case 1) and A′ ≡ d, B′ ≡ c (case 2). In both cases, the values obtained for $E^k_{(+)}$ and $E^k_{(-)}$ are rather small, implying a relatively even distribution among the three states. The best fit values for the energies and torsion angles, estimated using the empirical model analysis, are plotted in Figure 9. Good fits to the experimental data could be obtained for small values (<10°) of $\Delta\Phi$. Two example profiles for different values of $\Delta\Phi$ are shown in Figure 10. On the basis of the results presented in Figure 9, we have $E^k_{(-)} = E_{\sigma\alpha p} = 0.0 \pm 0.4$ kJ mol^{-1} and $E^k_{(+)} = E_{\sigma\beta p} = 1.0 \pm 0.4$ kJ mol^{-1} for case 1 and $E^k_{(+)} = E^k_{(-)} = E_{\sigma\alpha p} = E_{\sigma\beta p} = -1.1 \pm 0.4$ kJ mol^{-1} for case 2.

Higher Order Interactions. The analysis of the coupling constant data outlined above provides estimates for the conformational energies, $E_{\sigma\alpha}$, $E_{\sigma\beta}$, $E_{\sigma\alpha p}$, and $E_{\sigma\beta p}$. This procedure is based implicitly on the assumption that conformational probabilities for each bond are determined entirely by these first-order interaction energies (see eq 3). A more general treatment accounts for higher order interactions and requires considering the configuration of the entire chain. For an N segment chain, the probability that bond n is in state ν is

$$f^n_{(\nu)} = Z^{-1}\sum_{\phi_1}\cdots\sum_{\phi_n}\delta_{\nu\phi_n}\cdots\sum_{\phi_N} e^{-E(\phi_1\ldots\phi_n\ldots\phi_N)/kt} \qquad (4)$$

where Z is the conformational partition function, $E(\phi_1\ldots\phi_n\ldots\phi_N)$ is the energy of the chain in the conformation defined by the set of torsion angles $\phi_1\ldots\phi_n\ldots\phi_N$, and $\delta_{\nu\phi_n}$ is a Kronecker delta. In the first-order interaction approximation used above, the conformational energy is $E(\phi_1\ldots\phi_n\ldots\phi_N) = E_1(\phi_1) \ldots + \ldots E_n(\phi_n) \ldots + \ldots E_N(\phi_N)$.

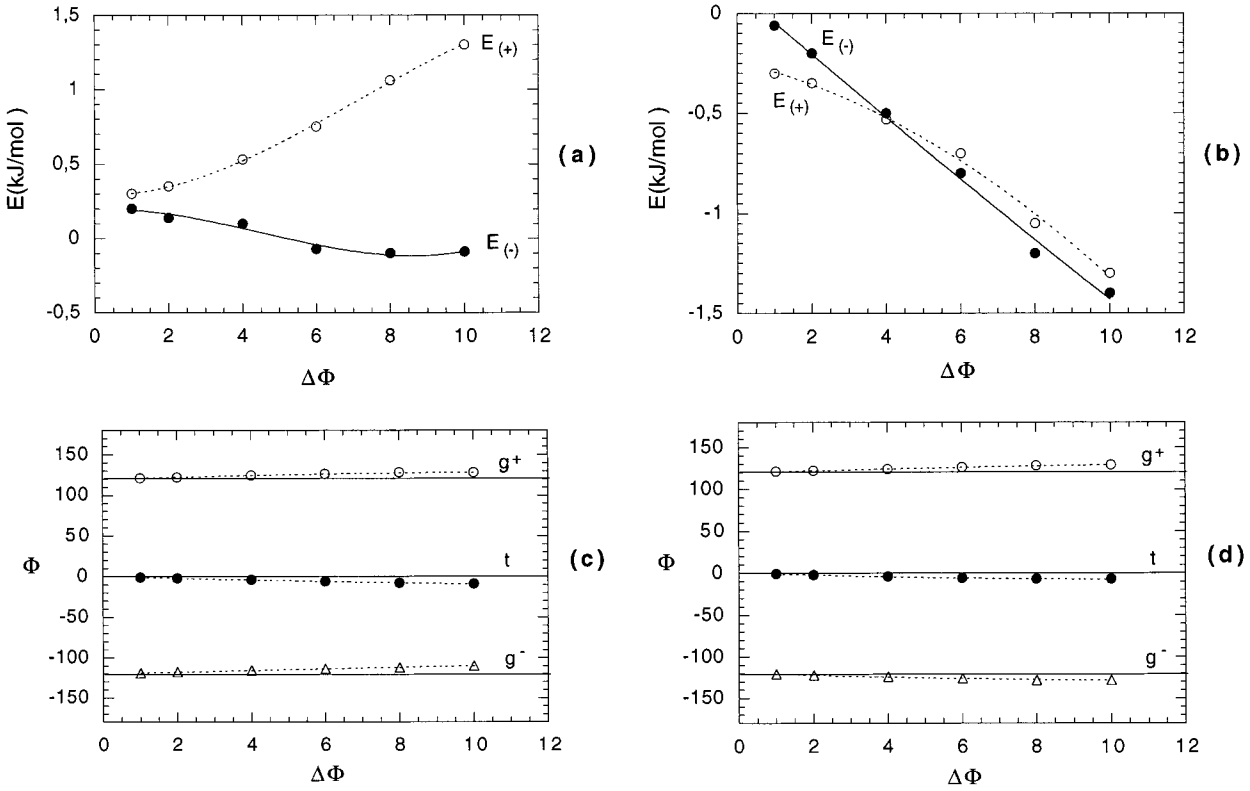

Figure 9. Best fit values of conformational energies, $E_{(+)}$ and $E_{(-)}$, as a function...maximum torsion angle distortion, $\Delta\Phi$, for bond k, assuming (a) case 1 and (b) case 2 NMR assignments. Below are shown best fit values for t, g^+, and g^- torsion angles for bond k assuming (c) case 1 and (d) case 2.

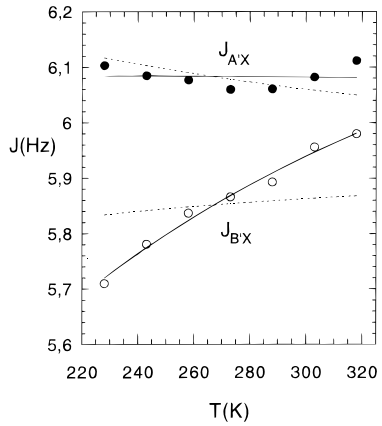

Figure 10. Best fit profiles for $J_{A'X}$ and $J_{B'X}$ for bond k obtained using the empirical model approach (see text). Filled circles and open circles refer experimental values for $J_{B'X}$ and $J_{A'X}$, respectively. Broken lines were obtained with $\Delta\Phi = 1°$. Solid lines are the best fit profiles with $\Delta\Phi = 10°$.

Evidently, in this limit, eq 4 and eq 3 are equivalent. Multiple summations such as those in eq 4 are conveniently expressed using matrix formalism,

$$f^{n}_{(\nu)} = Z^{-1}U_1[\prod_{i=2}^{n-1}U_i]u_{n\nu}[\prod_{i=n+1}^{N-1}U_i]U_N \qquad (5)$$

where U_1 and U_N are respectively row and column vectors with all elements equal to unity and U_i are statistical weight matrices for each bond i. The reduced matrix, $u_{n,\nu}$, for bond n has all columns equal to zero except that corresponding to state ν, whose elements are identical to those of the full matrix, U_n. Following the scheme presented in Figure 1b, the statistical weight matrices for bonds i, j, k, and l are (see following section)

$$U_i = \begin{bmatrix} 1 & 0 & \sigma'' \\ 1 & 0 & 0 \\ 1 & 0 & \sigma'' \end{bmatrix} \qquad U_j = \begin{bmatrix} 1 & \sigma_\alpha & \sigma_\beta \\ 0 & \sigma_\alpha & 0 \\ 1 & 0 & 0 \end{bmatrix}$$

$$U_k = \begin{bmatrix} 1 & \sigma_{\beta p} & \sigma_{\alpha p} \\ 1 & \sigma_{\beta p} & \omega\sigma_{\alpha p} \\ 1 & \omega\sigma_{\beta p} & \sigma_{\alpha p} \end{bmatrix} \qquad U_l = \begin{bmatrix} 1 & \sigma_k & \omega_{\eta k}\sigma'_k \\ 1 & \omega_{\eta k}\sigma_k & \omega_{\eta k}\sigma'_k \\ 1 & \omega_{\eta k}\sigma_k & \sigma'_k \end{bmatrix} \qquad (6)$$

Substitution of these matrices into eq 5 show that for bonds j and k, the populations of the individual states are given approximately (although not exactly) by the first-order terms, σ_α, σ_β and $\sigma_{\alpha p}$, $\sigma_{\beta p}$. The errors introduced in our estimates for the corresponding energies, $E_{\sigma\alpha}$, $E_{\sigma\beta}$, $E_{\sigma\alpha p}$, and $E_{\sigma\beta p}$, due to the neglect of higher order interactions (i.e., use of eq 3) are certainly much less than the errors deriving from approximations concerning the individual conformer coupling constants. A more detailed discussion of the use of NMR spectroscopy to investigate higher order interactions in PTMOTB is reserved for a future publication.[24]

(b) Dipole Moments. In the theoretical analysis of the polarity of the polymer, the C*(O*)−O ester groups (bonds a and d in Figure 1) were considered to be restricted to the trans states. The twist angle between aromatic rings in biphenyl type structures[25] is typically between 30° and 45°. For the purposes of the calculations here, torsion angles of 45, 135, 225, and 315° were employed for type b bonds. For bonds of type c only the conformations in which the carbonyl group is coplanar with the ester group are permitted and, consequently, the rotational angles about the bonds are 0 and 180°. The statistical weight matrices corresponding to skeletal bonds a through d are

$$U_a = [1], \qquad U_b = [1 \quad 1 \quad 1 \quad 1],$$

$$U_c = \begin{bmatrix} 1 & 1 \\ 1 & 1 \\ 1 & 1 \\ 1 & 1 \end{bmatrix}, \qquad U_d = \begin{bmatrix} 1 \\ 1 \end{bmatrix}$$

The rotational states about bonds of type e are located at 0, ±104°, and gauche states about these bonds have an energy, $E_{\sigma k}$, ca 1.7 kJ mol^{-1} above that of the alternative trans states.[26] Earlier studies carried out on the conformational properties of poly(ditrimethylene terephthalate) indicate that gauche states about CH_2-CH_2 bonds (bonds f and g) which give rise to $CH_2\cdots O$ first-order interactions, $E_{\sigma'}$, of ca. 0.4 kJ mol^{-1} below that of the corresponding trans states.[27] The rotational angles were considered to be 0, ±120°. The conformational analysis of polyoxides[1] shows that gauche states about bonds of type h are disfavored by $E_{\sigma''}$ of ca. 3.8 kJ mol^{-1} with respect to the alternative trans states and rotational angles about C−O bonds of the ether groups are 0, ±110°. Positive gauche states about bonds of type i give rise to strong repulsive interactions between methyl and methylene groups separated by four bonds, and the statistical weights of both g^+ and g^+g^+ states were assumed to be zero. For the same reason, the statistical weights of g^+t and g^-g^- states about bonds of type j are zero. Two sets of possible values for energies $E_{\sigma\alpha}$ and $E_{\sigma\beta}$ were obtained from the NMR analysis. For assignment case 1, $E_{\sigma\alpha} = E^j_{(+)} = 1.4 \pm 0.4$ kJ mol^{-1} and $E_{\sigma\beta} = E^j_{(-)} = 2.0 \pm 0.6$ kJ mol^{-1} and for case 2 we obtained $E^j_{(-)} = E_{\sigma\beta} = 0.5 \pm 0.3$ kJ mol^{-1} and $E^j_{(+)} = E_{\sigma\alpha} = -1.3 \pm 0.4$ kJ mol^{-1}. Similarly, for bond k, the analysis yielded the two sets of energies, $E_{\sigma\alpha p} = E^k_{(-)} = 0.0 \pm 0.30$ kJ mol^{-1} and $E_{\sigma\beta p} = E^k_{(+)} = 1.1 \pm 0.4$ kJ mol^{-1} for case 1 and $E_{\sigma\alpha p} = E_{\sigma\beta p} = E^k_{(+)} = E^k_{(-)} = -1.1 \pm 0.4$ kJ mol^{-1} for case 2. According to the NMR coupling constant analysis, the torsion angles deviate somewhat from their standard values, 0, ±120°. However, as discussed above, the calculations tend to overestimate the distortion of the main chain dihedral angles and in the absence of more detailed information regarding the individual conformer geometries, we have adopted the standard values in the calculations. The energy of g^+ states about bonds of type l is ca. 1.7 kJ mol^{-1} above that of the alternative trans state.[1] Due to strong repulsive second-order interactions between the $CH_3\cdots C^*(O^*)$ groups, the g^- state is much less favored than the g^+ state. An energy $E_{\sigma' k} = 6$ kJ mol^{-1} was tentatively used in the calculations. The statistical weight matrices for bonds i through l are given above (see eq 6). Energies associated with second-order interactions O···O, $CH_2\cdots O$, and $C^*(O^*)\cdots CH_2$, represented by $E_{\omega'}$, E_ω, and $E_{\omega\eta k}$, were considered to be 2.5, 2.5, and 4.8 kJ mol^{-1} above that of the tt states.[28]

The dipole corresponding to the $C_6H_5-COOCH_2$ group, μ_E, has a value of 1.89 D and forms an angle of 123° with the $C^{ar}-C^*(O^*)$ bond.[29] The dipole associated with the ether bonds has a value of 1.07 D and lies along the C−O bond.[28] All CH_2-CH_2 were considered to possess zero dipole moments. Values of the mean square dipole moment, $\langle\mu^2\rangle$ of the chains were calculated by standard matrix multiplication methods described in detail elsewhere. The results obtained for $\langle\mu^2\rangle$ are expressed in terms of the intramolecular dipolar correlation coefficient,

$$g = \frac{\langle\mu^2\rangle}{2x(\mu_E{}^2 + \mu_{C-O}{}^2)} \tag{7}$$

where x is the degree of polymerization and μ_E and μ_{C-O} are respectively the dipoles associated with the ester group and the ether CH_2-O bond. Because the polymers have high molecular weights, chain end-group effects have been neglected. Strictly speaking, PTOMTB chains are random copolymers in which the acid residue may be flanked by the following segments: $-CH_2CH_2-CH_2O-$, $-CH_2CH(CH_3)CH_2O-$, or $-CH_2CH_2CH_2O-/-CH_2CH(CH_3)CH_2O-$. However, preliminary calculations show that the mean-square dipole moment of the chains is not sensitive to the comonomers distribution. Consequently, subsequent calculations were performed by considering the chains as homopolymers with the repeating unit indicated in Figure 1.

For chains in the all-trans conformation with all bond dipoles lying in a plane, the total dipole should be close to zero. However, because the aromatic rings in the biphenyl group are twisted relative to each other, the overall planarity is lost and the value for g is 0.029. Departures from the trans conformation arising from rotations about the bonds of the glycol residue, increase $\langle\mu^2\rangle$ and, consequently, the value of the dipolar correlation coefficient. Note that for uncorrelated dipoles, g takes the value of 1. Model calculations have been performed with the set of conformational energies, $E_{\sigma k} = 1.3$, $E_{\sigma' k} = 6.3$, $E_{\sigma''} = 3.8$, $E_{\sigma'} = -0.4$, $E_\omega = 2.5$, and $E_{\omega\eta k} = 8.4$ kJ mol^{-1}, and the energies $E_{\sigma\alpha}$, $E_{\sigma\beta}$, $E_{\sigma\alpha p}$, and $E_{\sigma\beta p}$, for bonds j and k obtained from the NMR coupling constant analysis. For each series of calculations, one energy value was varied while all others were maintained fixed at their initial values. Because the NMR analysis provides two sets of values for each pair of energies, $E_{\sigma\alpha}$, $E_{\sigma\beta}$, and $E_{\sigma\alpha p}$, $E_{\sigma\beta p}$, there are a total of four possible combinations of parameters. Figure 11 shows the variation of the dipolar correlation coefficient, g, for two of these combinations. Results are displayed for the dependence of g on $E_{\sigma''}$, $E_{\sigma'}$, $E_{\sigma\alpha}$, and $E_{\sigma\beta}$, the mean square dipole moment being rather insensitive to other energy terms. The first series of calculations (open circles and broken lines) correspond to the initial energies $E_{\sigma\alpha} = 1.4$, $E_{\alpha\beta} = 2.0$ kJ mol^{-1} and $E_{\sigma\alpha p} = 0.0$, $E_{\sigma\beta p} = 1.0$ kJ mol^{-1}. The second series of calculations (filled circles with solid lines) were performed using the same values of $E_{\sigma\alpha p}$ and $E_{\sigma\beta p}$ but with the bond j energies, $E_{\sigma\alpha} = -1.3$, $E_{\sigma\beta} = 0.5$ kJ mol^{-1}, corresponding to assignment case 2 in the NMR analysis. The horizontal line at $g = 0.73$ is the experimental value measured for PTMOTB in dioxane at 303 K. Vertical lines denote the standard values of the energy parameters (see discussion above) derived from previous studies or from the NMR analysis in this work. For the first set of energy values (open circles), the calculated value of g is 0.68, somewhat lower than the experimental value. Even allowing for a reasonable margin of error in each of the conformational energies about their "standard" values, it is not possible to reproduce the experimental result. In contrast, the second combination of energies ($E_{\sigma\alpha} = -1.3$ kJ mol^{-1}, $E_{\sigma\beta} = 0.5$ kJ mol^{-1}) gives $g = 0.74$, in excellent agreement with experiment. Unfortunately, the dipole moment is rather insensitive to $E_{\sigma\alpha p}$ and $E_{\sigma\beta p}$, and it has not been possible to establish precise values for these quantities. However, comparison of the results obtained here for PTOMTB with those of previous studies (see below) lends support to the assignment $E_{\sigma\alpha p} = 0.0$, $E_{\sigma\beta p} = 1.0$

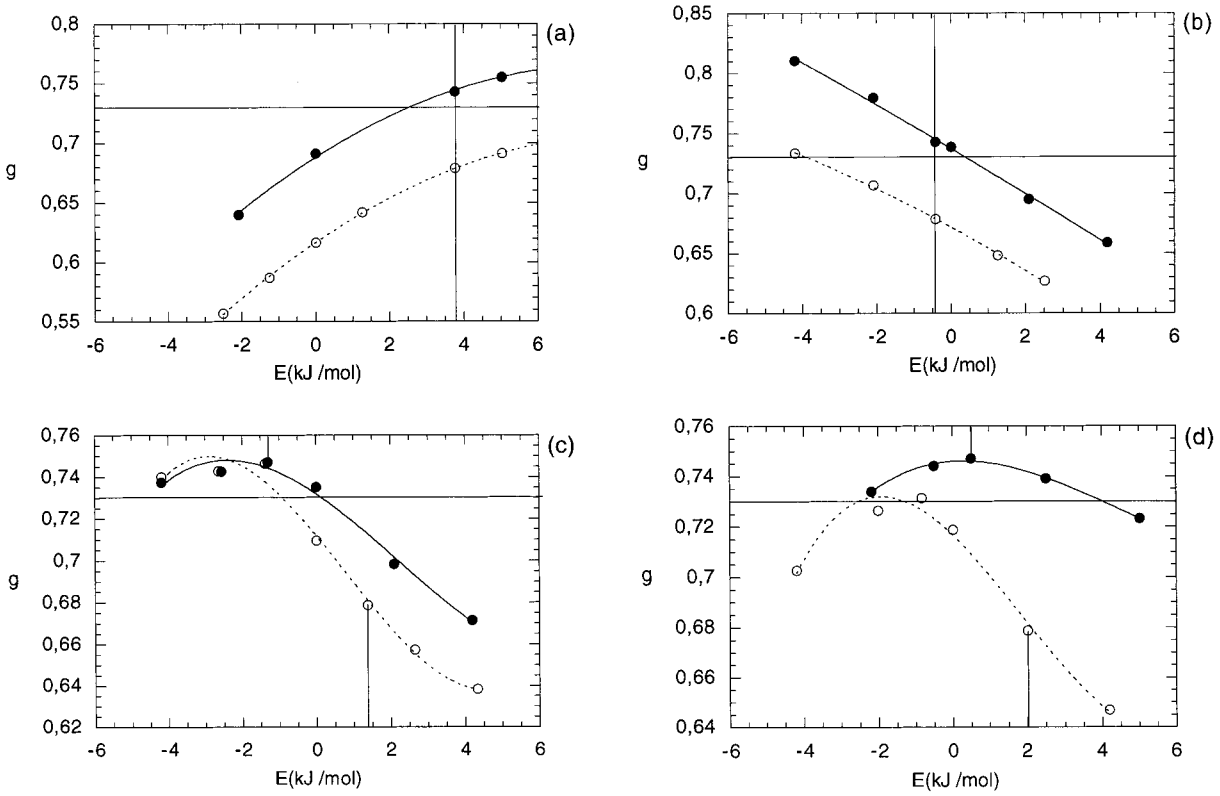

Figure 11. Variation of the dipolar correlation coefficient, g, calculated for PTMOTB as a function of conformational energies for different bonds in the glycol spacer. The profiles in each plot show the change in g as one energy is...varied independently, with all others fixed at their "standard" values. Results are shown for (a) $E_{\sigma''}$, (b) E_{σ}', (c) $E_{\sigma\alpha}$, and (d) $E_{\sigma\beta}$. Horizontal solid lines correspond to the experimental value, $g = 0.73$. Solid vertical lines in each plot refer to the standard value of the varied energy parameter. Open circles refer to calculations performed with standard values for the energies, $E_{\sigma k} = 1.3$, $E_{\sigma' k} = 6.3$, $E_{\sigma''} = 3.8$, $E_{\sigma'} = -0.4$, $E_{\omega} = 2.5$, $E_{\omega\eta k} = 8.4$, $E_{\sigma\alpha} = 1.4$, $E_{\sigma\beta} = 2.0$, $E_{\sigma\alpha p} = 0.0$, and $E_{\sigma\beta p} = 1.0$ kJ mol^{-1}. Filled circles refer to calculations performed using $E_{\sigma\alpha} = -1.3$ and $E_{\sigma\beta} = 0.5$ kJ mol^{-1} and with all other energies the same as for the previous calculations.

kJ mol^{-1} used to obtain the results in Figure 11. Of the remaining energies, it is $E_{\sigma''}$ and E_{σ}' that exert the greatest influence on the dipole moment. The polarity of the chain decreases as the gauche population about C−C bonds of the glycol residue diminishes. Increasing $E_{\sigma'}$ from −4 to +4 kJ mol^{-1} causes g to decrease from 0.80 to 0.67. Conversely, the chain polarity is found to increase as the gauche states of C−O bonds become less populated. In fact, g increases from 0.64 to 0.77 as $E_{\sigma''}$ varies from −2 to +8 kJ mol^{-1}.

It is interesting to compare the results obtained here for the conformational energies of the bonds flanking the asymmetric carbon with those found for poly(3-methyloxetane) (P3MO) whose repeating unit is $-CH_2-CH(CH_3)CH_2O-$.[30] In P3MO, gauche states about $CH_2CH(CH_3)-CH_2O$ bonds that bring an oxygen atom between a methyl and a methylene group have an energy ca. 1.30 kJ mol^{-1} below that of the corresponding trans state, while those conformations that result in single gauche interactions between an oxygen atom and a methylene group have an energy ca. 2.1 kJ mol^{-1} below that of the trans. The preference for gauche states in substituted oxetanes mainly arises from attractive Coulombic interactions between the negative residual charge of the oxygen atom and the positive residual charge of the carbon atom of the methylene group bonded to the oxygen atom of the previous repeating unit. This effect appears to be diminished significantly in the case of PTOMTB where gauche states of bonds containing the asymmetric carbon have somewhat higher energies than the corresponding states in P3MO. Presumably, this reflects a reduced charge separation between the methylene carbon and the attached oxygen of the ester group. Thus, in PTOMTB, energy differences between gauche and trans states in the $-OCH_2CH(CH_3)CH_2O-$ unit are reduced relative to those in P3MO, implying a greater flexibility in this segment.

.Summarizing, we have employed NMR spectroscopy and dipole moment studies to determine the conformational distribution of bonds neigboring the asymmetric carbon in the mesogenic polymer PTOMTB. On the basis of the dipole moment analysis, it is possible to distinguish between two possible assignments for the NMR spectra and hence determine unambiguously the conformational energies for one of these bonds, namely bond j containing the ether linkage. Specifically, the values derived are $E_{\sigma\beta} = 0.5 \pm 0.3$ kJ mol^{-1} and $E_{\sigma\alpha} = -1.3 \pm 0.4$ kJ mol^{-1}. The rather low values for the conformational energies of bond k (adjacent to the ester linkage) and the relative insensitivity of the dipole moment to these energies preclude unambiguous assignment for the conformational energies of this bond. However, by inference from the results obtained for bond j and their interpretation in terms of Coulombic interactions, we tentatively adopt the values $E_{\sigma\alpha p} = 0.0 \pm 0.30$ and $E_{\sigma\beta p} = 1.1 \pm 0.4$ kJ mol^{-1}.

References and Notes

(1) Flory, P. J. *The Statistical Mechanics of Chain Molecules*; Wiley: New York, 1969.
(2) Volkenstein, V. *Conformational Characteristics of Polymer Chains*; Interscience: New York, 1963.

(3) Riande, E.; Saiz, E. *Dipole Moments and Birefringence of Polymers*; Prentice Hall: Englewood Cliffs, NJ, 1992.
(4) Mattice, W. L.; Suter, U. W. *Conformations of Large Molecules: The Rotational.Isomeric State Model in Macromolecules*; Wiley-Interscience: New York, 1994.
(5) Mizushima, S. *Structure of Molecules and Internal Rotations*; Academic Press: New York, 1954.
(6) Orville-Thomas, J., Ed. *Internal Rotations in Molecules*; Wiley-Interscience: New York, 1974.
(7) Gutowsky, H. S.; Belford, G. G.; McMahon, P. E. *J. Chem. Phys.* **1962**, *36*, 3353.
(8) Matsuzaki, K.; Hiroshi, I. L. *J. Polym. Sci., Polym. Phys. Ed.* **1974**, *17*, 883.
(9) Viti, V.; Indovina, P. L.; Podo, F.; Radics, L.; Némethy, G. *Mol. Phys.* **1974**, *27*, 541.
(10) San Roman, J.; Guzmán, J.; Riande, E.; Santoro, J.; Rico, M. *Macromolecules* **1982**, *15*, 609.
(11) Riande, E.; Jimeno, M. L.; Salvador, R.; de Abajo, J.; Guzmán, J. *J. Phys. Chem.* **1990**, *94*, 7435.
(12) Karplus, M. J. *Chem. Phys.* **1959**, *30*, 11.
(13) Haasnoot, C. A. G.; de Leeuw, F. A. M.; Altona, C. *Tetrahedron* **1980**, *36*, 2783.
(14) Tasaki, K.; Abe, A. *Polym. J.* **1985**, *17*, 641.
(15) Abe, A.; Tasaki, K.; Mark, J. E. *Polym. J.* **1985**, *17*, 883.
(16) Inomata, K.; Abe, A. *J. Phys. Chem.* **1992**, *96*, 7934.
(17) Ferrarini, A.; Luckhurst, G. R.; Nordio, P. L. *Mol. Phys.* **1995**, *85*, 131.
(18) Serpi. H. S.; Photinos, D. J. *J. Chem. Phys.* **1996**, *105*, 1718.
(19) Clark, N. A.; Lagerwall, S. T. *Appl. Phys. Lett.* **1980**, *36*, 899
(20) Uchida, S.; Morita, K.; Miyoshi, K.; Hashimoto, K.; Kawasaki, K. *Mol. Cryst. Liq. Cryst.* **1988**, *155*, 93.
(21) Bovey, F. A. *Nuclear Magnetic Resonance Spectroscopy*; Academic Press: San Diego, 1988.
(22) Guggenheim, E. *Trans. Faraday Soc.* **1949**, *45*, 714; **1951**, *47*, 573.
(23) Smith, J. W. *Trans. Faraday Soc.* **1950**, *46*, 394.
(24) Heaton, N. J.; Bello, P.; Riande, E. Manuscript in preparation.
(25) Veracini, C. A.; Longeri, M. In *Nuclear Magnetic Resonance of Liquid Crystals*; Emsley, J. W., Ed.; Reidel: Dordrecht, The Netherlands, 1985; p 123.
(26) Riande, E. *J. Polym. Sci., Polym. Phys. Ed.* **1977**, *15*, 1397.
(27) Gonzalez, C.; Riande, E.; Bello, A.; Pereña, J. M. *Macromolecules* **1988**, *21*, 3230.
(28) Abe. A.; Mark, J. E. *J. Am. Chem. Soc.* **1976**, *98*, 6468.
(29) Saiz, E.; Hummel, J. P.; Flory, P. J.; Plavsic, M. *J. Phys. Chem.* **1981**, *85*, 3211.
(30) Riande, E.; de la Campa, J. G.; Guzmán, J.; de Abajo, J. *Macromolecules* **1984**, *17*, 1431.

MA970813G